Electronic Supplementary Material (ESI) for Physical Chemistry Chemical Physics.

In Silico Capture and Activation of Methane with Light Atom Molecules

Stefan Mebs,[1]* Jens Beckmann[2]

[1] *Institut für Experimentalphysik, Freie Universität Berlin, Arnimallee 14, 14195 Berlin, Germany*

[2] *Institut für Anorganische Chemie und Kristallographie, Universität Bremen, Leobener Straße 7, 28359 Bremen, Germany*

Supporting Information

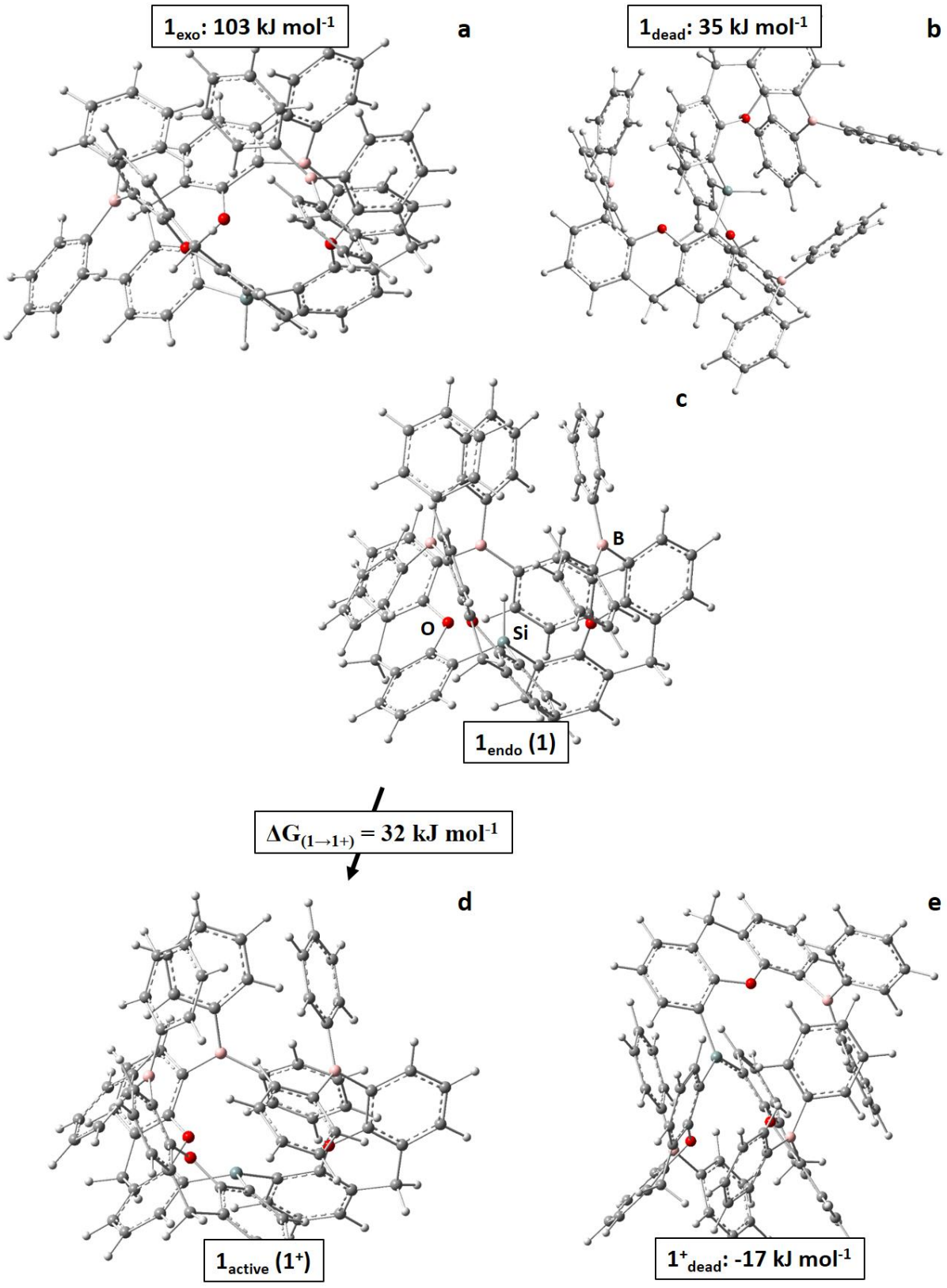

Figure S1. Structures and relative energies (ΔE) or enthalpies (ΔG) of $\mathbf{1}_{exo}$ (**1**) (a), $\mathbf{1}_{dead}$ (b), $\mathbf{1}_{endo}$ (**1**) (c), $\mathbf{1}^{+}_{active}$ ($\mathbf{1}^{+}$) (d), and $\mathbf{1}^{+}_{dead}$ (e).

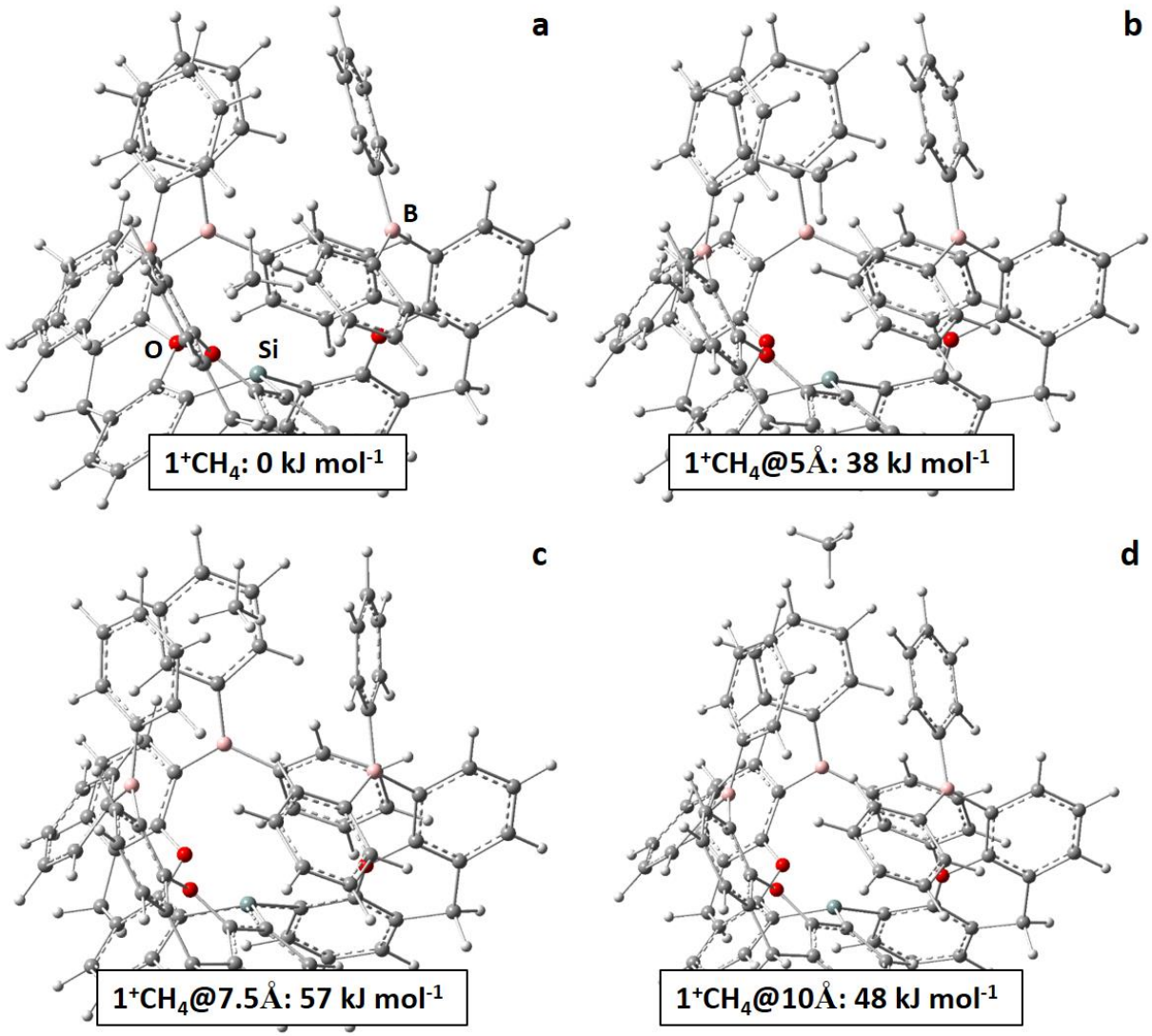

Figure S2. Structures and relative energies (ΔE) of **1⁺CH₄** (a), and **1⁺CH₄** at fixed Si···C distances of 5.0 Å (b), 7.5 Å (c), and 10.0 Å (d).

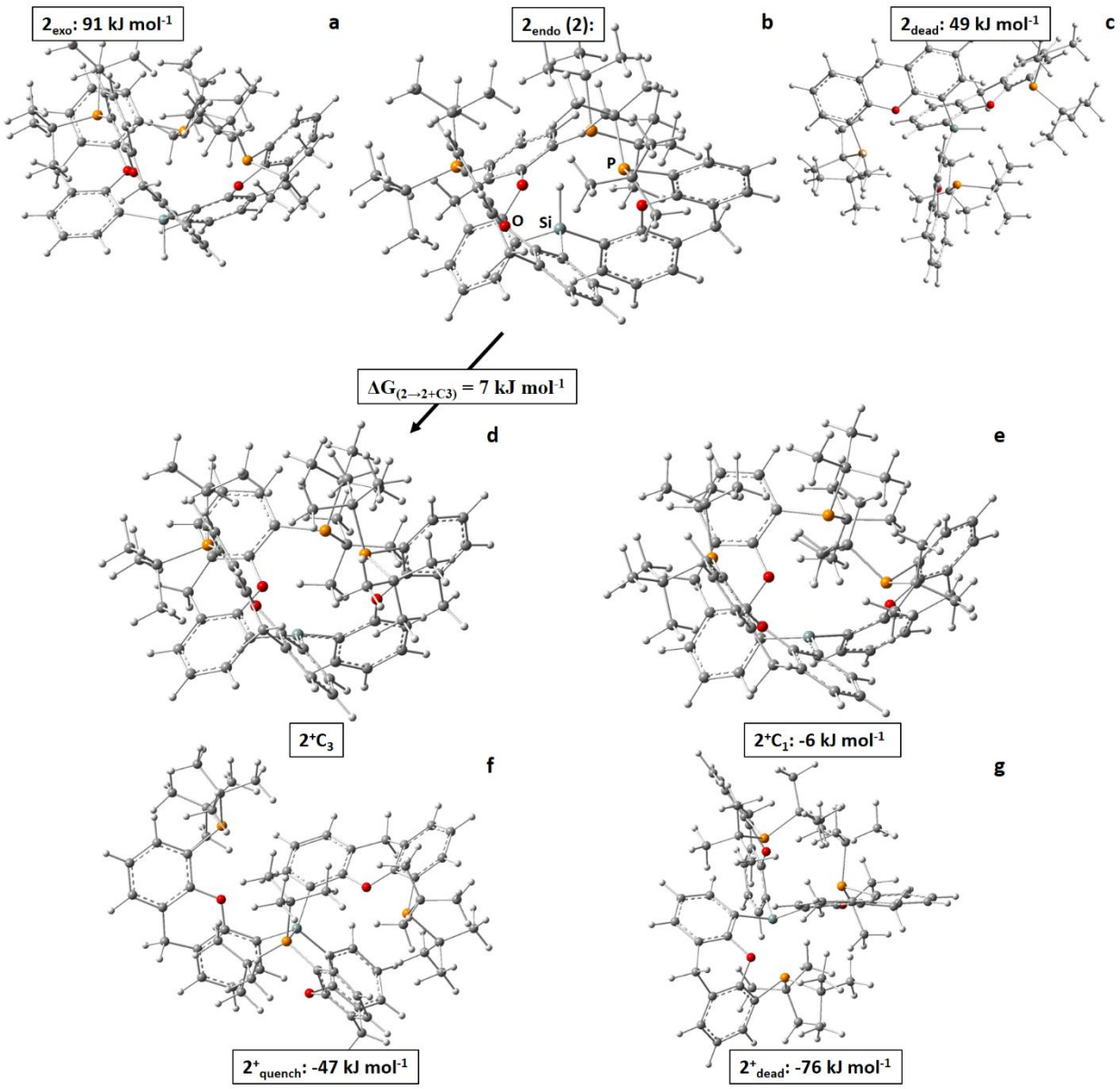

Figure S3. Structures and relative energies (ΔE) or enthalpies (ΔG) of $\mathbf{2}_{exo}$ (a), $\mathbf{2}_{endo}$ (**2**) (b), $\mathbf{2}_{dead}$ (c), $\mathbf{2}^{+}\mathbf{C}_3$ (d) , $\mathbf{2}^{+}\mathbf{C}_1$ (e) , $\mathbf{2}^{+}_{quench}$ (f) , and $\mathbf{2}^{+}_{dead}$ (g).

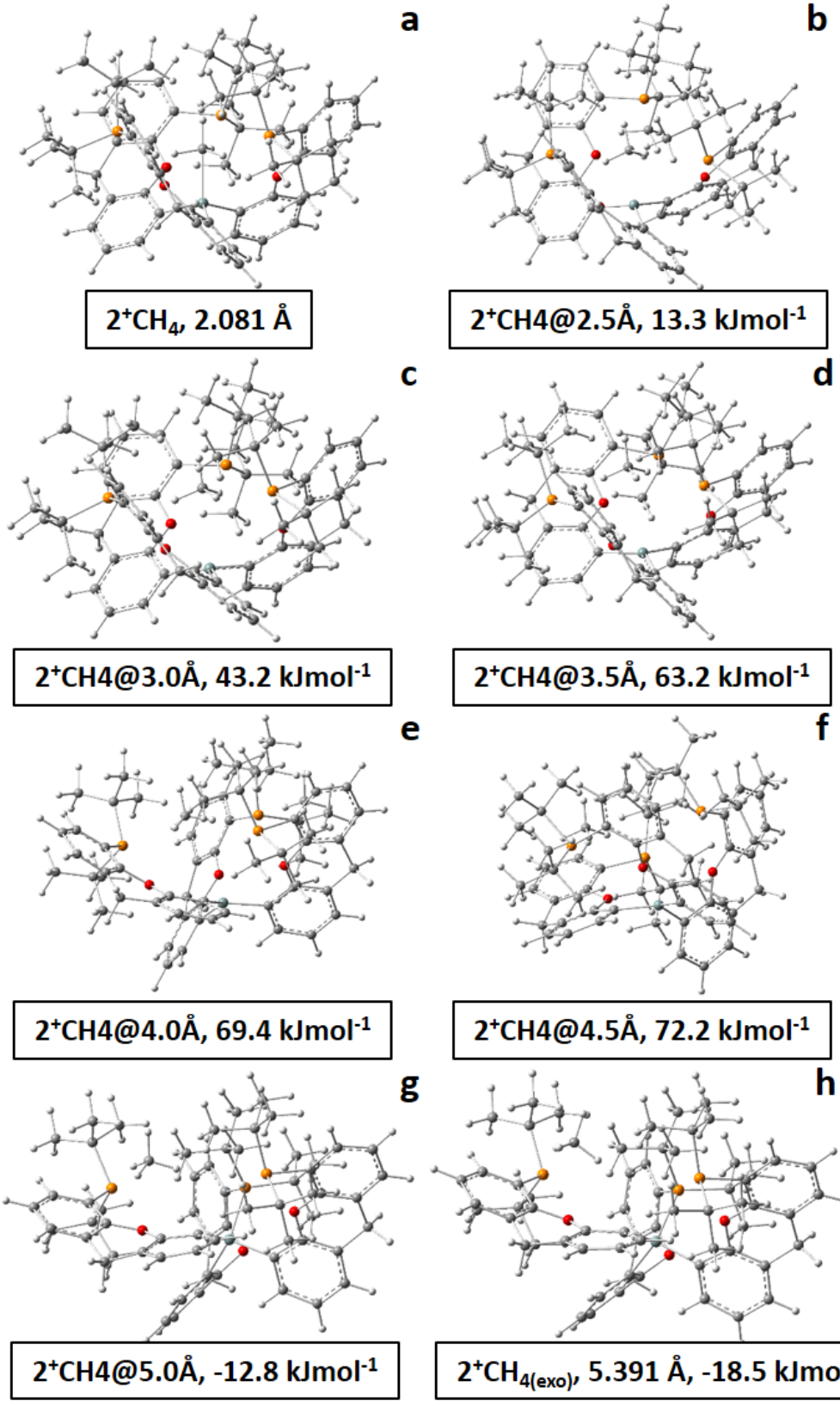

Figure S4. Structures and relative energies (ΔE) of **2⁺CH₄** (a), and **2⁺CH₄** at fixed Si···C distances of 2.5-5.0 Å (b-g), (h) free optimization with CH_4 fragment outside the void.

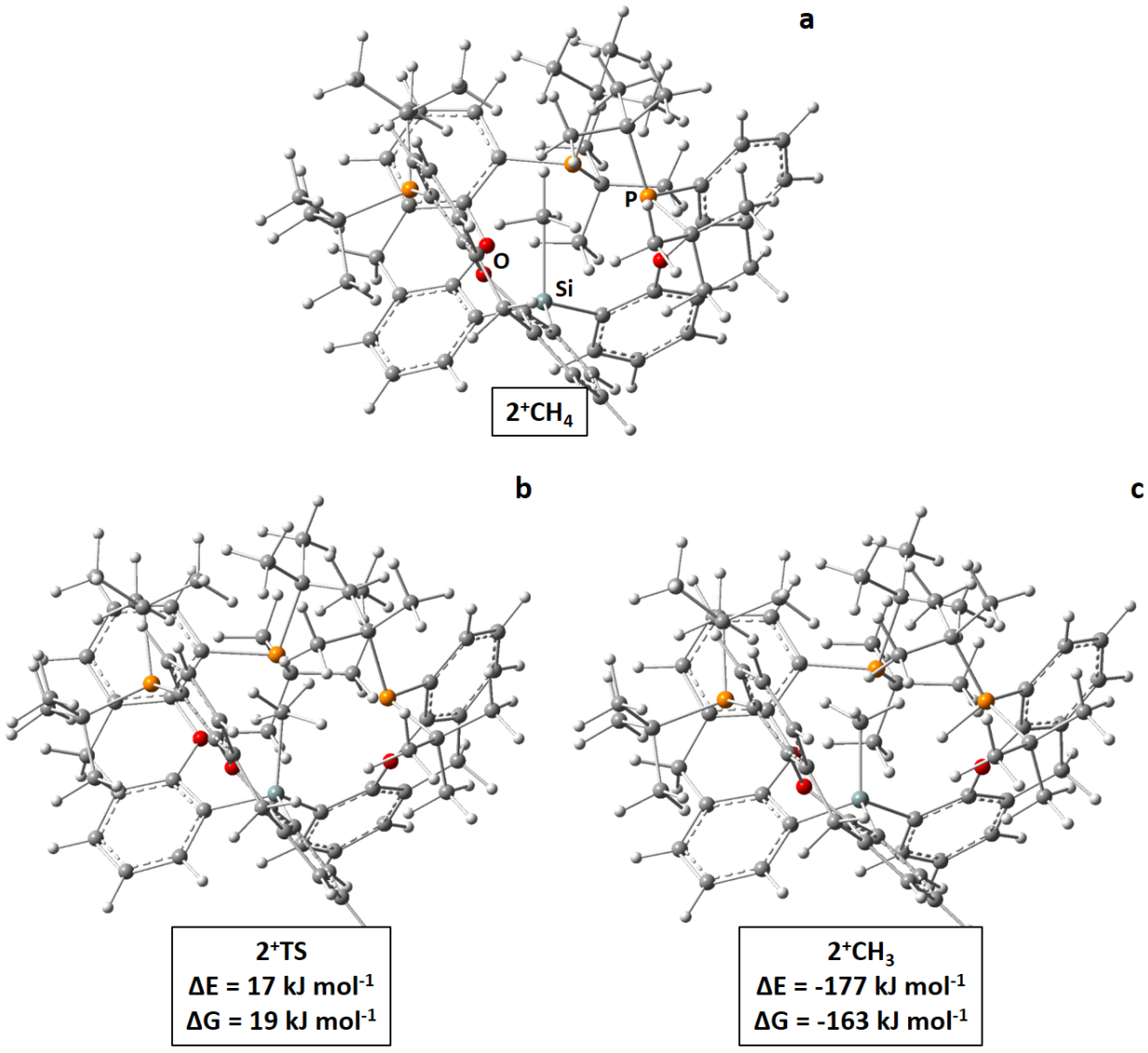

Figure S5. Structures and relative energies (ΔE) and enthalpies (ΔG) of **$2^{+}CH_4$** (a), **2^{+}TS** (b), and **$2^{+}CH_3$** (c).

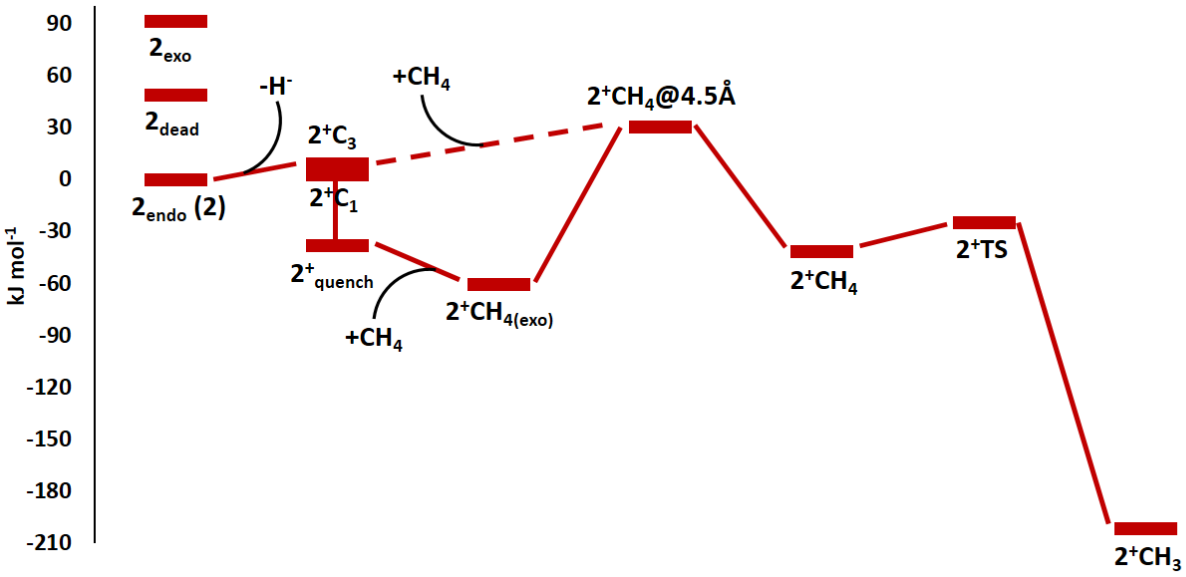

Figure S6. Relative energies (ΔE, dark red) of structural isomers (e.g. exo-, dead-, and endo-variants of the neutral starting state **2**, the activated states of $\mathbf{2}^{+}$, or the methane complex, $\mathbf{2}^{+}\mathbf{CH_4}$, with the CH_4-fragment at different $Si^{\cdots}CH_4$ distances, the transition-state towards deprotonation ($\mathbf{2}^{+}\mathbf{TS}$), as well as the final complex with a $Si–CH_3$ and a $HP_{xan}tBu_2$ group ($\mathbf{2}^{+}\mathbf{CH_3}$). Due to the complexity of the scheme, no ΔG values are displayed, and ΔE values for the methane complexes are not corrected for BSSE or the 1-atm-to-1-M conversion. The scheme thus serves a rather qualitative picture of complex formation and structural transformations. Starting from the neutral $\mathbf{2}_{\mathbf{endo}}$ (**2**) as the likely main product of ligand synthesis, hydride abstraction is almost energy neutral, providing $\mathbf{2}^{+}\mathbf{C_3}$. Unfortunately, there is no energy barrier for $\mathbf{2}^{+}\mathbf{C_3}$ to directly convert into $\mathbf{2}^{+}\mathbf{C_1}$ and finally into $\mathbf{2}^{+}$**quench**, which has a short Si–P bond. Adding CH_4 gas may cause formation of a methane adduct in which CH_4 resides at the outer parts of the charged ligand, $\mathbf{2}^{+}\mathbf{CH_{4(exo)}}$, from which a considerable energy barrier of circa 90 kJ mol^{-1} has to be overcome to form the desired methane complex $\mathbf{2}^{+}\mathbf{CH_4}$. It is yet unclear of purging **2** with pressurized CH_4 gas *via* hydrogen abstraction may give access to a shortcut (dashed line), preventing quenching of the system. Once the C_3-symmetric $\mathbf{2}^{+}\mathbf{CH_4}$ is formed, the ligand exerts an exit-barrier, which is significantly larger than the transition-state towards deprotonation, ultimately forming an $Si\text{-}CH_3$ complex.

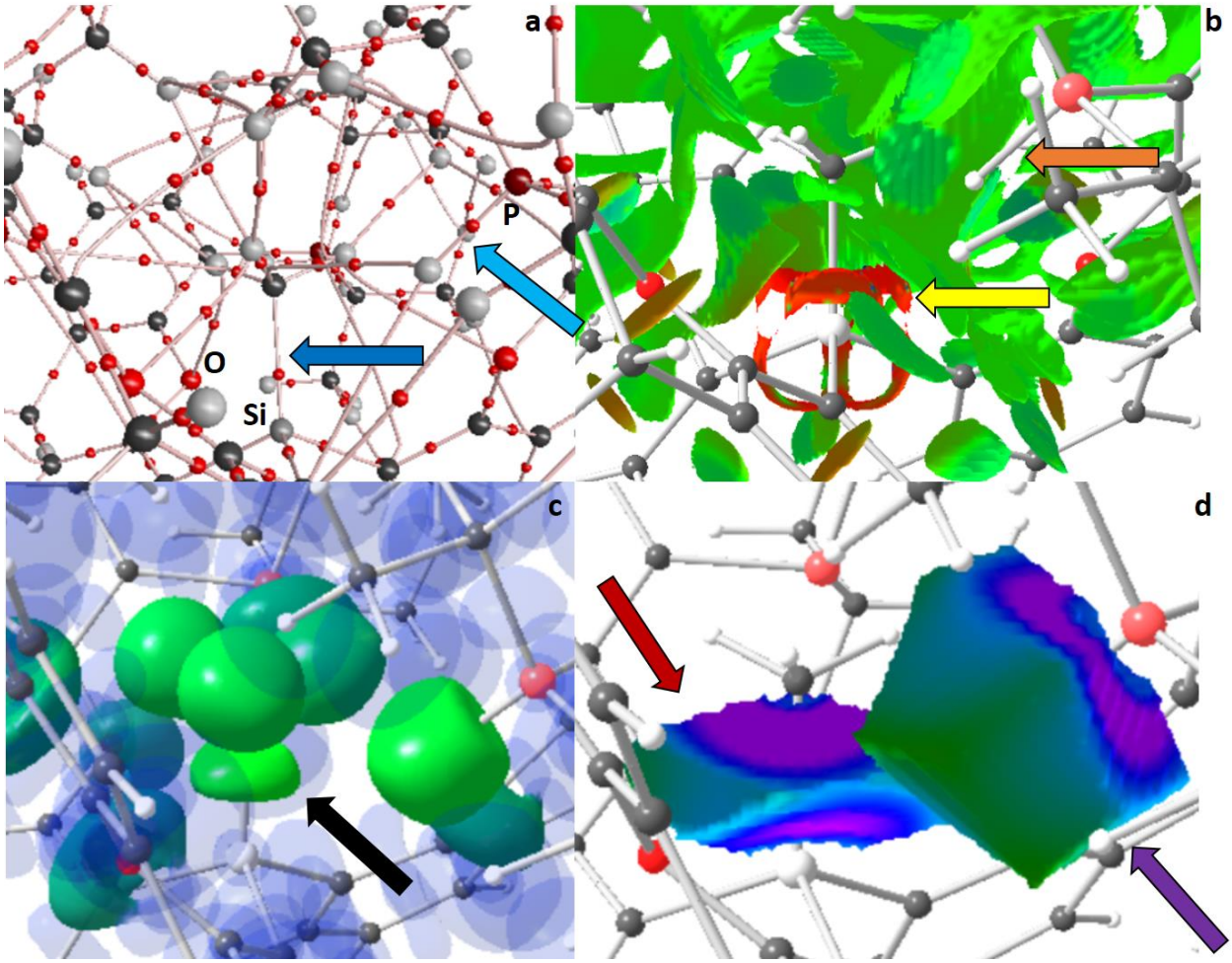

Figure S7. RSBI analysis of $\mathbf{2^{+}CH_3}$ (a) AIM bond paths motif, (b) NCI *iso*-surface at s(r) = 0.5, (c) ELI-D localization domain representation at an *iso*-value of 1.4, (d) ELI-D distribution mapped on the Si–C_{CH4} ELI-D bonding as well as on the H basin of the H atom being transferred to the P atom. Color code atoms: hydrogen – light gray, carbon – medium gray, oxygen – medium red, phosphor – dark or pale red.

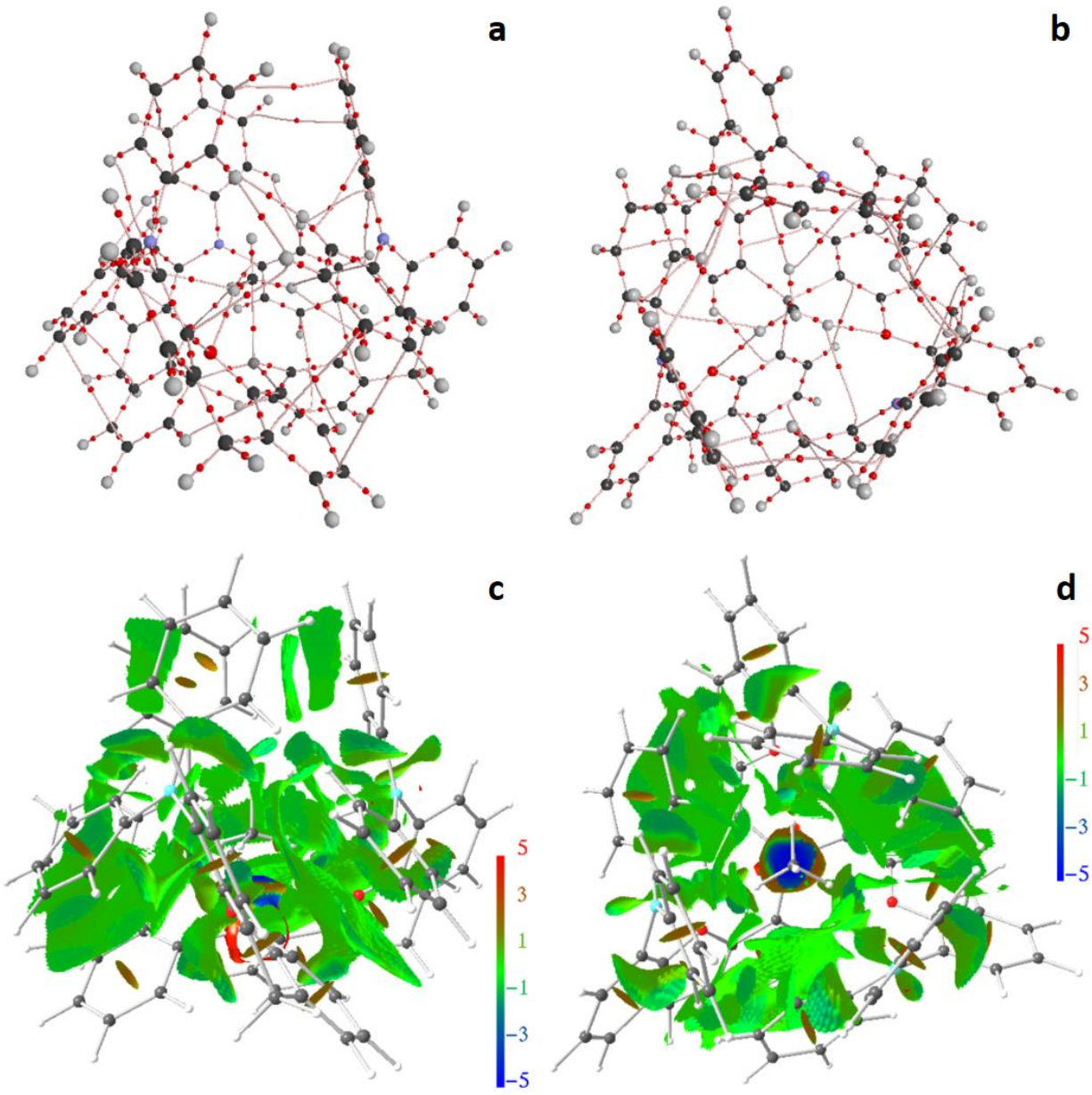

Figure S8. RSBI analysis (side and top views) of **1**$^{+}$**CH**$_4$ (a,b) AIM bond paths motif, (c,d) NCI *iso*-surface at s(r) = 0.5. The Si–C NCI domain is disc-shaped, indicating dominance of ionic bond contributions. The molecule complies C3-symmetry.

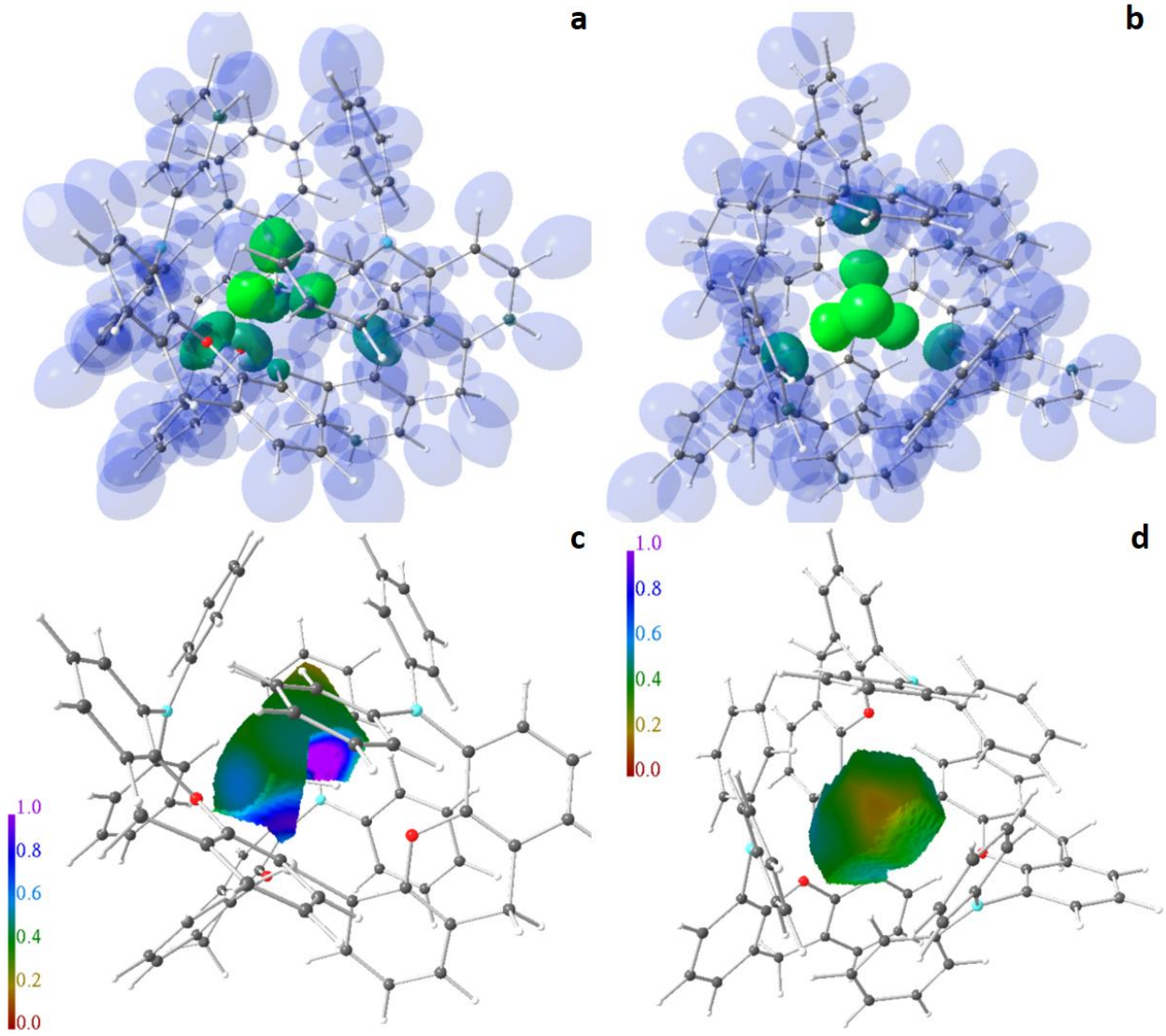

Figure S9. RSBI analysis (side and top views) of **$1^{+}CH_4$** (a,b) ELI-D localization domain representation at an *iso*-value of 1.4, (c,d) ELI-D distribution mapped two H_{CH4} ELI-D basins (equatorial and axial). The purple-colored excrescence towards the Si atom (center of part c) indicates the pre-formation of a separate Si–C ELI-D bonding basin and thus the uprise of covalent bond contributions.

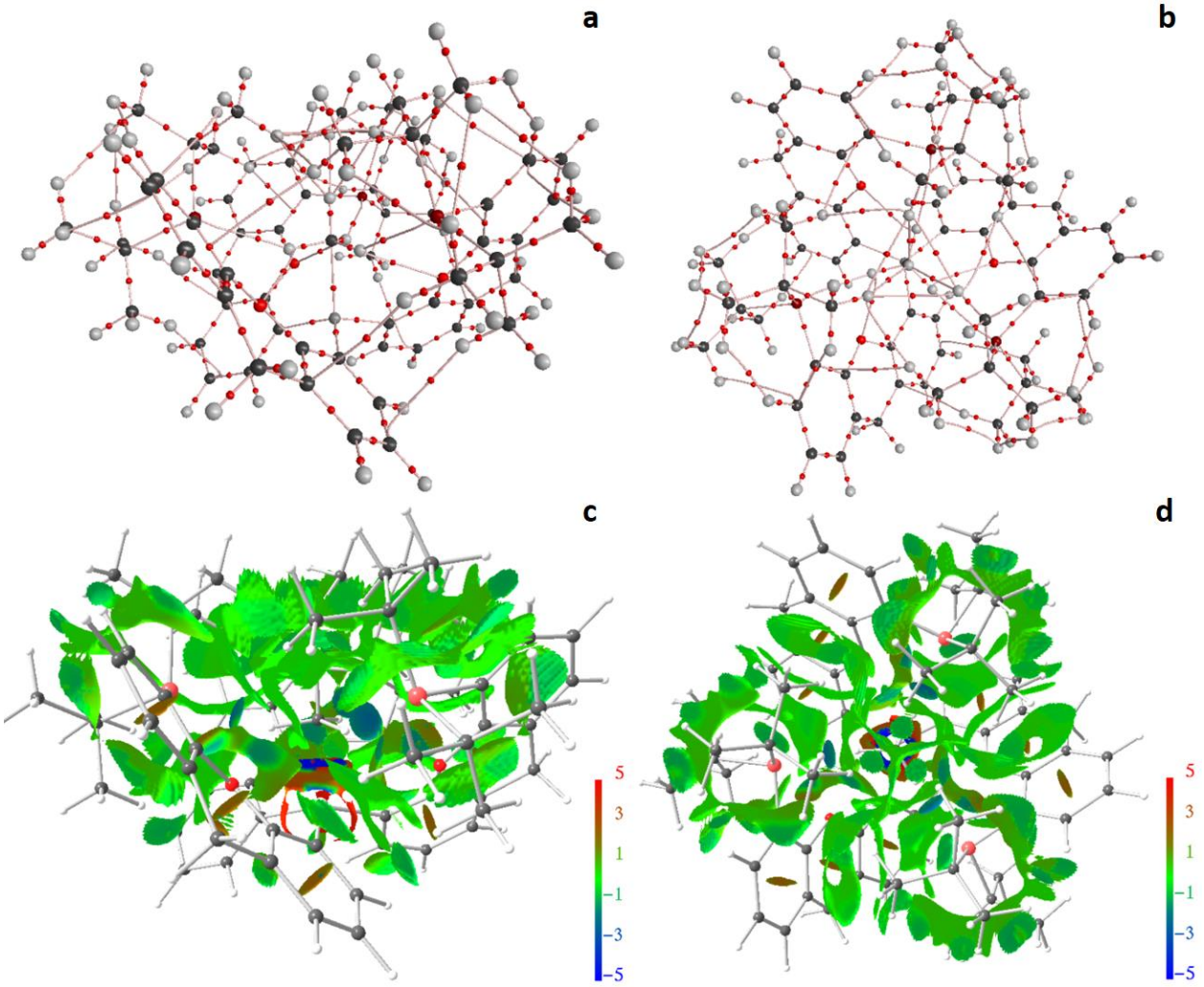

Figure S10. RSBI analysis (side and top views) of **$2^{+}CH_4$** (a,b) AIM bond paths motif, (c,d) NCI *iso*-surface at s(r) = 0.5. The Si–C NCI domain is ring-shaped, indicating coexistence of ionic and covalent bond contributions. The molecule complies C3-symmetry.

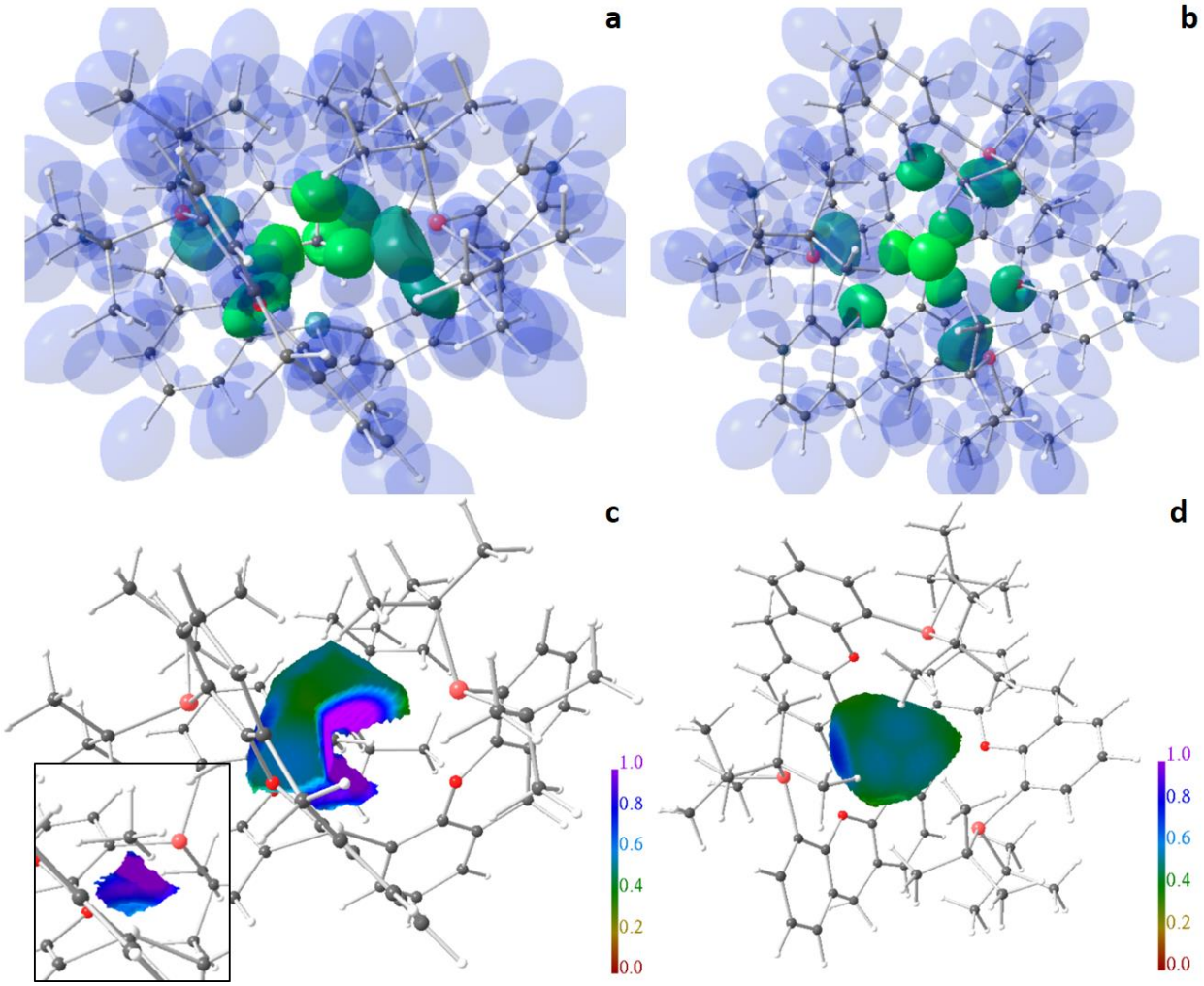

Figure S11. RSBI analysis (side and top views) of **$2^{+}CH_4$** (a,b) ELI-D localization domain representation at an *iso*-value of 1.4, (c,d) ELI-D distribution mapped on the small Si–C ELI-D bonding basin as well as on two H_{CH4} basins (equatorial and axial). The inset in part c displays the topologically separated Si–C ELI-D bonding basin highlighting the relevance of covalent bond contributions to this interaction.

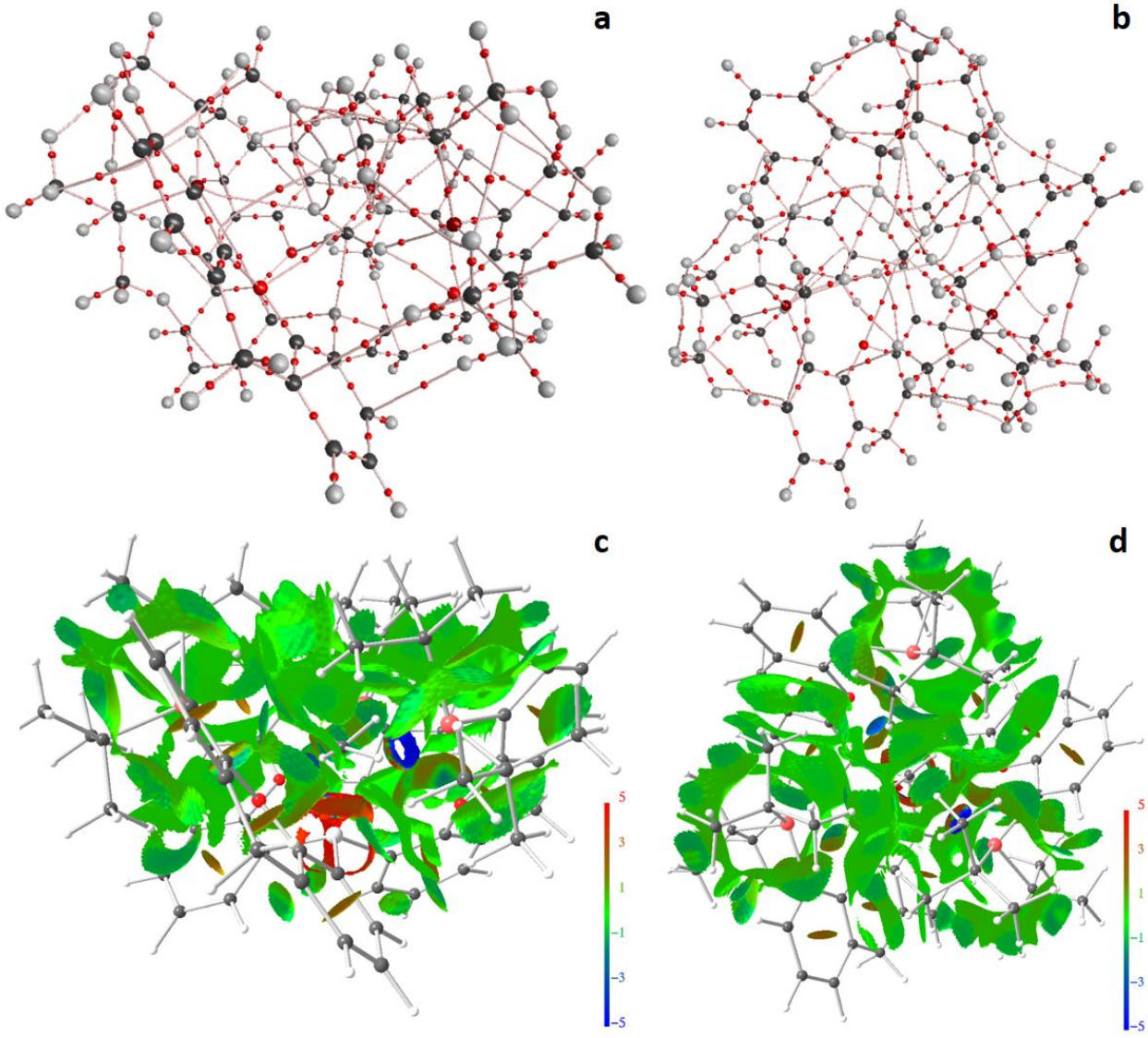

Figure S12. RSBI analysis (side and top views) of **2^{+}TS** (a,b) AIM bond paths motif, (c,d) NCI *iso*-surface at s(r) = 0.5. A ring-shaped P$^{\cdots}$H$_{CH4}$ NCI domain is formed.

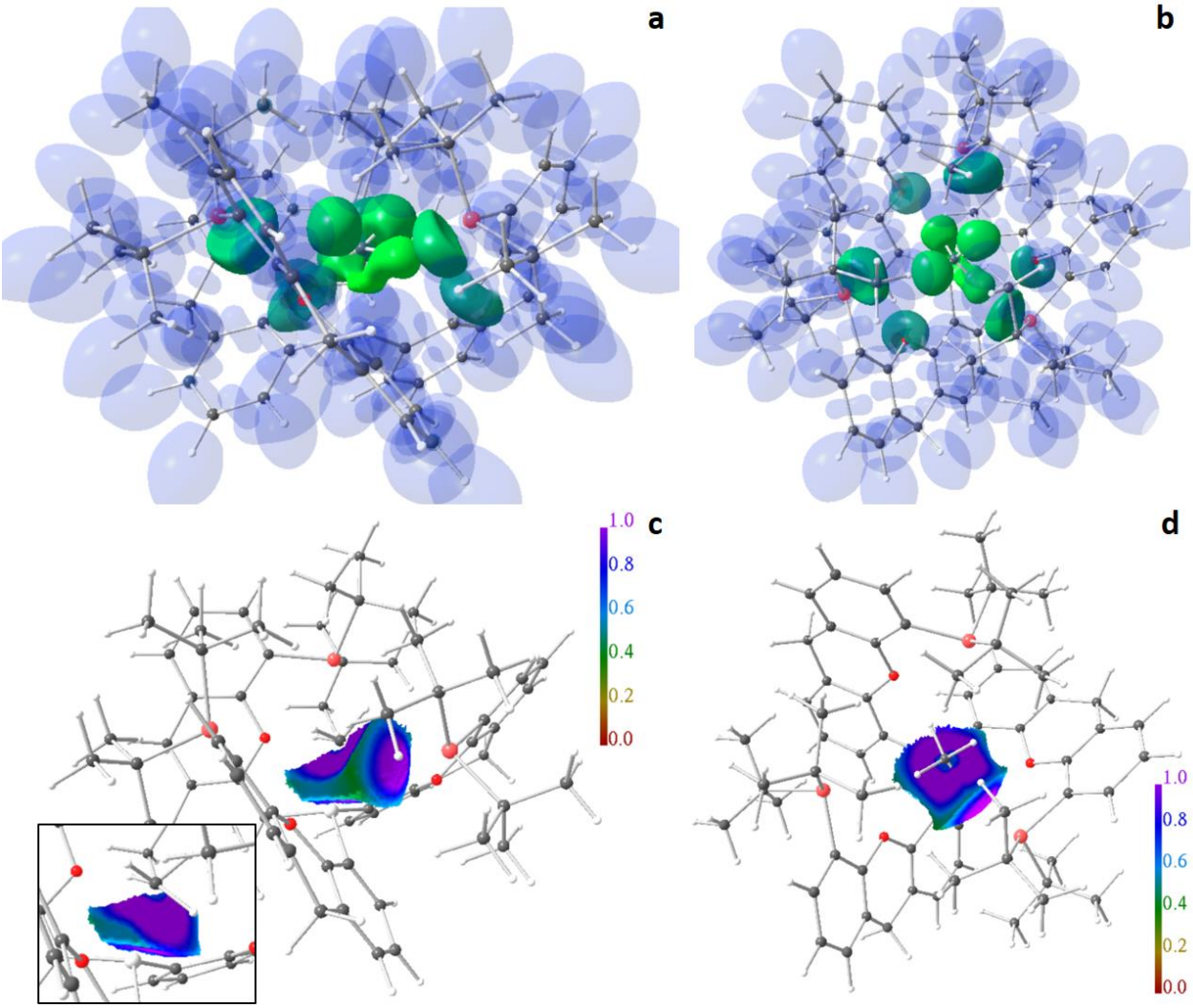

Figure S13. RSBI analysis (side and top views) of **2^{+}TS** (a,b) ELI-D localization domain representation at an *iso*-value of 1.4, (c,d) ELI-D distribution mapped on the Si–C ELI-D bonding basin as well as on the H_{CH4} basins (equatorial) of the transferred H atom. The inset in part c displays the Si–C ELI-D bonding basin highlighting the relevance of covalent bond contributions to this interaction.

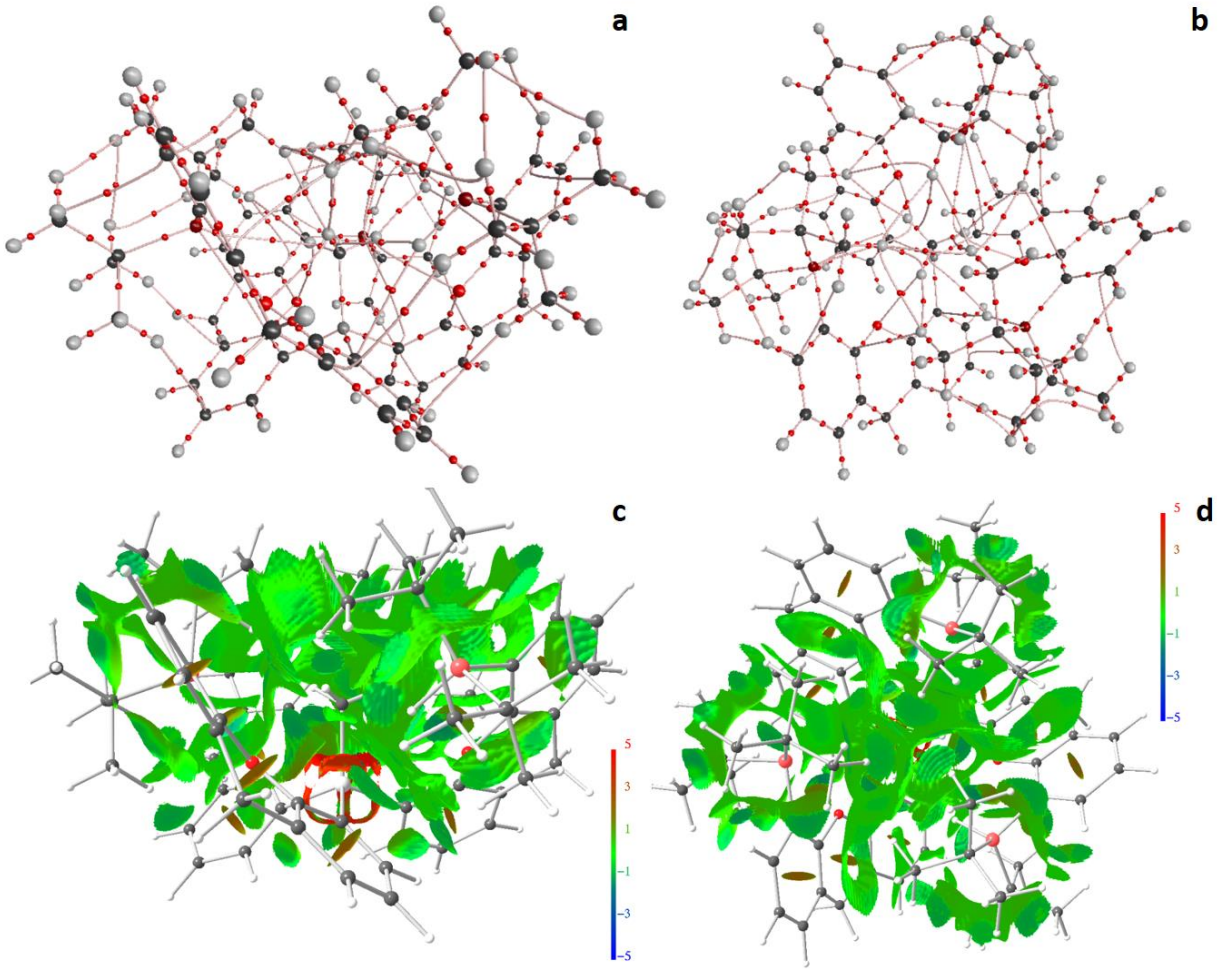

Figure S14. RSBI analysis (side and top views) of $\mathbf{2^{+}CH_3}$ (a,b) AIM bond paths motif, (c,d) NCI *iso*-surface at s(r) = 0.5. The NCI top view shows that the void-space around the Si–CH_3 part is "closed" again as it is fully covered by green H···H contact patches.

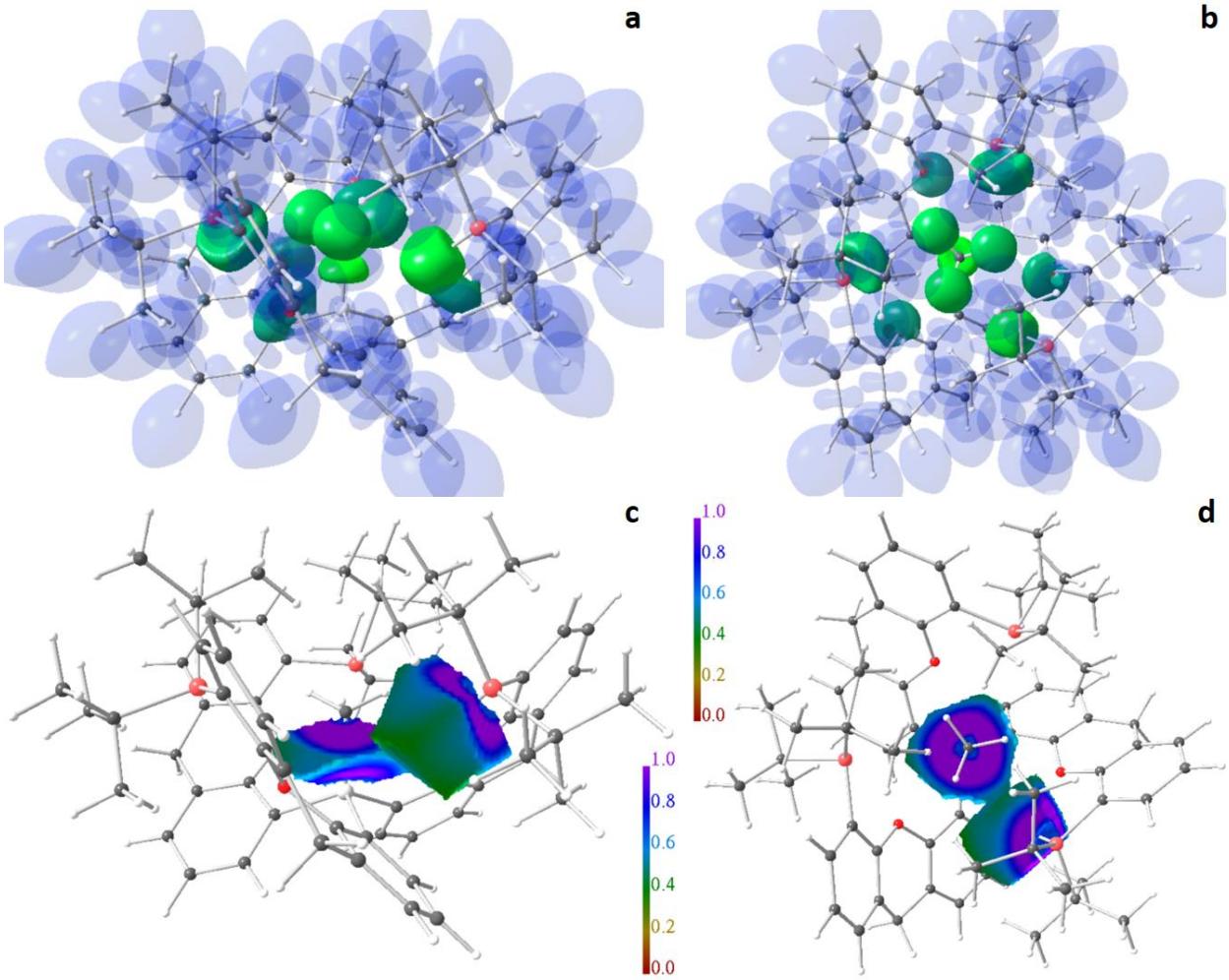

Figure S15. RSBI analysis (side and top views) of **$2^{+}CH_3$** (a,b) ELI-D localization domain representation at an *iso*-value of 1.4, (c,d) ELI-D distribution mapped on the Si–C ELI-D bonding basin as well as on the H_{CH4} basin (equatorial) of the transferred H atom, which is now attached to the P atom.

Table S1. Relative energies (ΔE) and enthalpies (ΔG) of relevant states and transitions

	1	**1**$^{\&}$	**2**	**2**$^{\&}$	type	comment
exo	103.4	98.5	91.2	84.5	ΔE	relative to endo
endo						
dead	35.2	35.1	48.7	46.8	ΔE	relative to endo
active	27.1	21.6	8.9	0.3	ΔE	endo → active
	31.5		7.0		ΔG	endo → active
complex	-43.1	-52.2	-37.1 (9.8)$^{\$}$	-50.2(-14.0)	ΔE	active → complex
	4.2		7.1 (35.5)$^{\$}$		ΔG§	active → complex
enter	2.2	1.6	69.0	67.6	ΔE	relative to **1**$^{+}$ or **2**$^{+}$ + CH_4
trap	57.2	64.8	72.2	74.2	ΔE	relative to **1**$^{+}$**CH**$_4$ or **2**$^{+}$**CH**$_4$
2^{+}**TS**			18.8	20.3	ΔG	**2**$^{+}$**CH**$_4$ → **2**$^{+}$**TS**
2^{+}**CH**$_3$			–181.5	-170.3	ΔG	**2**$^{+}$**TS** → **2**$^{+}$**CH**$_3$

"exo": neutral ligand system with Si–H in exo-position; "endo": neutral ligand system with Si–H in endo-position; "dead": neutral ligand system in unfavorable conformation; "active": charged species (**1**$^{+}$ or **2**$^{+}$**C**$_3$; $: numbers in brackets for **2** use **2**$^{+}_{\textbf{quench}}$ as reference); "complex": CH_4-complexes (**1**$^{+}$**CH**$_4$ or **2**$^{+}$**CH**$_4$; ΔG§ values are corrected for BSSE (4.0 or 5.6 kJ mol^{-1}) and 1-atm-to-1-M conversion (7.9 kJ mol^{-1})); "enter": estimated energy barrier to enter the void – for **1**$^{+}$**CH**$_4$ this refers to a Si···C distance of 7.5 Å, for **2**$^{+}$**CH**$_4$ this refers to a Si···C distance of 4.5 Å; "trap": estimated energy barrier to leave the void after complex formation; TS: transition state; &: single-point calculations at the higher 6-311+G(2df,p) basis-set using the structural coordinates of the optimizations conducted using the 6-31+G* basis-set; corresponding BSSE-values are 3.0 and 3.4 kJ mol^{-1}.

Table S2. Thermodynamic parameters.

model	$^{+}CPh_3$	$HCPh_3$	**1**	$\mathbf{1}^{+}$	**2**	$\mathbf{2}^{+}C_3$
E (a.u.)	-732.6888	-733.4911	-3480.2067	-3479.3940	-3986.8901	-3986.0843
ZPVE (kcal/mol)	176.8140	183.1631	686.3394	682.5798	800.4500	795.4848
ZPE-corr (H/n)	0.2818	0.2919	1.0938	1.0878	1.2756	1.2677
TD-E corr	0.2963	0.3069	1.1582	1.1523	1.3470	1.3393
TD-H corr	0.2972	0.3079	1.1592	1.1532	1.3480	1.3402
TD-G corr	0.2395	0.2468	0.9937	0.9882	1.1748	1.1668
E+ZPE	-732.4070	-733.1993	-3479.1130	-3478.3063	-3985.6145	-3984.8166
E+TD-E	-732.3925	-733.1842	-3479.0485	-3478.2418	-3985.5430	-3984.7450
E+TD-H	-732.3915	-733.1833	-3479.0476	-3478.2408	-3985.5421	-3984.7441
E+TD-G	-732.4493	-733.2444	-3479.2130	-3478.4059	-3985.7153	-3984.9175
E-TD (Kcal/Mol)	185.9	192.6	726.8	723.1	845.3	838.6
CV (Cal/molK)	59.1	60.0	263.0	262.7	287.7	280.8
S (Cal/molK)	121.5	128.6	348.2	347.3	264.5	280.4

model	$\mathbf{2}^{+}_{quench}$	CH_4	$\mathbf{1}^{+}CH_4$	$\mathbf{2}^{+}CH_4$	$\mathbf{2}^{+}TS$	$\mathbf{2}^{+}CH_3$
E (a.u.)	-3986.1022	-40.5069	-3519.9207	-4026.6104	-4026.6041	-4026.6777
ZPVE (kcal/mol)	797.6287	28.2112	712.3010	824.0968	823.1824	825.9928
ZPE-corr (H/n)	1.2711	0.0450	1.1351	1.3133	1.3118	1.3163
TD-E corr	1.3414	0.0478	1.2031	1.3876	1.3847	1.3889
TD-H corr	1.3424	0.0488	1.2041	1.3886	1.3856	1.3898
TD-G corr	1.1739	0.0276	1.0327	1.2113	1.2121	1.2165
E+ZPE	-3984.8311	-40.4619	-3518.7856	-4025.2971	-4025.2923	-4025.3613
E+TD-E	-3984.7608	-40.4590	-3518.7176	-4025.2228	-4025.2194	-4025.2888
E+TD-H	-3984.7598	-40.4581	-3518.7167	-4025.2218	-4025.2185	-4025.2878
E+TD-G	-3984.9283	-40.4792	-3518.8880	-4025.3991	-4025.3920	-4025.4611
E-TD (Kcal/Mol)	841.8	30.0	755.0	870.8	868.9	871.5
CV (Cal/molK)	285.5	6.5	274.0	297.5	294.7	293.2
S (Cal/molK)	354.7	44.5	360.6	373.2	365.2	364.7

Scheme S1: Potential synthesis route for **1**

Dichloromethane would be the typically used solvent as it doesn't quench the Lewis acidic sites (as donor solvents, such as THF, ethers etc., but also electron rich aromatic solvents, such as toluene, benzene etc. would do). A proposed reaction pathway for the preparation of the host system is outlined as follows:

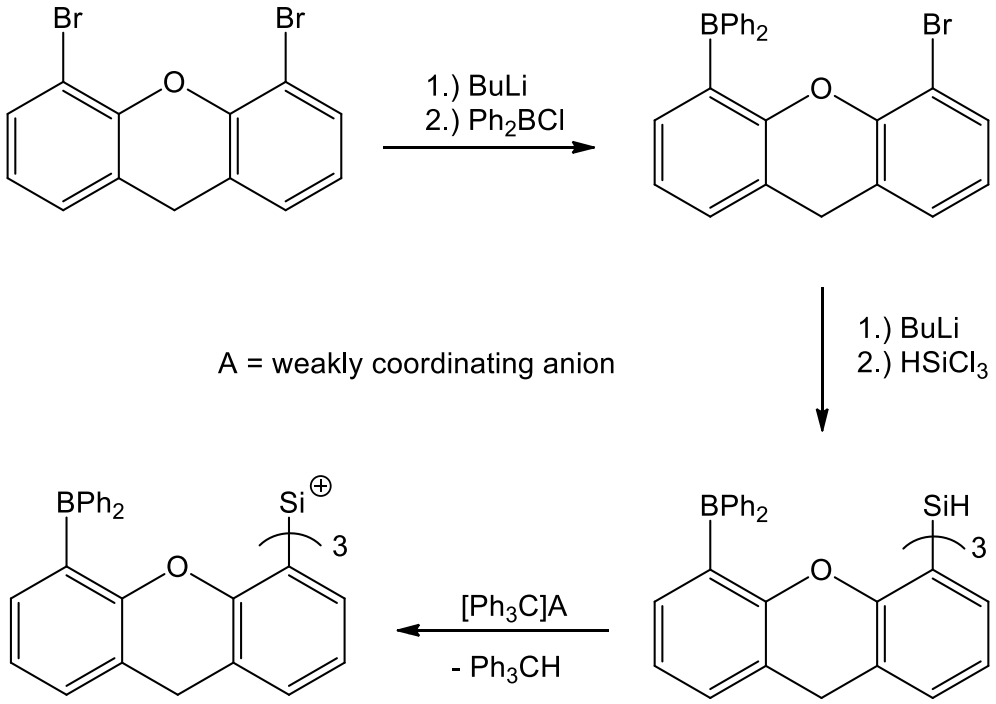

All steps involve common reagents and conditions typically employed in synthetic organometallic chemistry.